A Model for the Evolution of Network Dislocation Density in Irradiated Metals

F.A. Garner and W.G. Wolfer

September 1982

UWFDM-484

ASTM-STP-782, 1073-1087 (1982).

FUSION TECHNOLOGY INSTITUTE

UNIVERSITY OF WISCONSIN

MADISON WISCONSIN

A Model for the Evolution of Network Dislocation Density in Irradiated Metals

F.A. Garner and W.G. Wolfer

Fusion Technology Institute
University of Wisconsin
1500 Engineering Drive
Madison, WI 53706

http://fti.neep.wisc.edu

September 1982

UWFDM-484

ASTM-STP-782, 1073-1087 (1982).

A MODEL FOR THE EVOLUTION OF NETWORK DISLOCATION DENSITY IN IRRADIATED METALS

F.A. Garner*
W.G. Wolfer

Fusion Engineering Program
Nuclear Engineering Department
University of Wisconsin
Madison WI 53706

September 1982

UWFDM-484

*Hanford Engineering Development Laboratory, Richland WA.

A MODEL FOR THE EVOLUTION OF NETWORK DISLOCATION DENSITY IN IRRADIATED METALS

F. A. Garner (Hanford Engineering Development Laboratory) and W. G. Wolfer (University of Wisconsin)

ABSTRACT: It is well-known that the total dislocation density that evolves in irradiated metals is a strong function of irradiation temperature. The dislocation density comprises two components, however, and only one of these (Frank loops) retains it temperature dependence at high fluence. The network dislocation density approaches a saturation level which is relatively insensitive to starting microstructure, stress, irradiation temperature, displacement rate and helium level. The latter statement is supported in this paper by a review of published microstructural data. It is shown that the influence of surface proximity can obscure the independence of temperature and displacement rate however.

A model has been developed to explain the insensitivity to many variables of the saturation network dislocation density. This model does not assume random motion of dislocations by climb and glide but takes into account the correlated nature of dislocation components in a dense array. The model also explains how the rate of approach to saturation can be sensitive to displacement rate and temperature while the saturation level itself is not very dependent on these variables. It is predicted that the insensitivity of ρ_d^* to temperature will persist until thermal emission of vacancies from network dislocations becomes important. At higher displacement rates typical of charged particle simulation experiments, the temperature at which thermally-induced climb of dislocations becomes important is increased as both the point defect and microstructural densities undergo an upward shift with displacement rate.

1 Introduction

When metals are irradiated at elevated temperatures with fast neutrons or charged particles to large damage levels, a substantial restructuring of their microstructure occurs. One facet of this evolution is the development of a dislocation microstructure composed of network dislocations and various types of dislocation loops. Although it is well known that the total dislocation line length is often a strong function of temperature, it now appears that in bulk material only the Frank loop component retains its temperature dependence at high fluence. It also appears that the network component of the dislocation microstructure approaches a saturation level which is remarkably insensitive to the starting microstructure and to many material and environmental variables.

The temperature independence of the saturation level can be obscured in charged particle irradiations where the influence of the surface is large. This report examines the available data to assess the validity of the concept of saturation density. A model is then developed to explain this behavior.

It was shown earlier that in AISI 316 all microstructural components (voids, loops, network dislocations, precipitates) approach saturation levels during irradiation.[1-3] With the exception of network dislocations, all are known to be sensitive to temperature, stress and displacement rate. Helium and other gases are known to affect the density of voids and sometimes the early evolution of Frank loops. The orientation of the latter is also quite sensitive to the magnitude and spatial orientation of the stress state.[4-8]

Since the radiation-induced dislocation loops are the major source of radiation-induced network line length, it may appear surprising at first that the parametric sensitivities of dislocation loops are not expressed in their progeny. Examination of loop behavior during irradiation will provide the insight needed to explain this apparent anomaly.

2 Evolution of Dislocation Loop Microstructure

To this point we have addressed dislocation loops in general terms only. There is a variety of loops which may form, but the major contributors are Frank loops composed of platelets of interstitial atoms lying parallel to the close-packed planes of the crystalline matrix. Frank loops composed of vacancies have been observed to form simultaneously with interstitial loops but usually occur only in well-annealed materials at low fluence and prior to the extensive formation of network dislocations.[1] Si-Ahmed and Wolfer have explained this observation in terms of the relative point defect capture efficiencies of both types of Frank loops and that of network dislocations.[9]

Although Frank interstitial loops can unfault and the resultant loops rotate to other orientations, it is the sessile nature of the Frank loop that limits the rate of evolution of the dislocation microstructure. While other dislocation components can glide as well as climb, the Frank loop can only extend its boundaries and increase its line length by net absorption of interstitial atoms.

It is also important to note that while the loops are the primary source of new line length, the size distribution and density of Frank loops are controlled just

as strongly by the density and mobility of the network dislocations. This has been demonstrated in several studies that show that the size distribution of loops is controlled not only by their growth rate but also by the probability that the loops will unfault upon intersection with other dislocation components.[5,8]

When loops grow in the relatively open spaces of annealed material, they tend to overshoot the saturation level characteristic of the temperature and displacement rate as shown in Figure 1. Once the loops start to intersect, however, the "oversized" loop distribution is rapidly reduced in both mean size and density, approaching the same level imposed on loops which evolve in dense networks of dislocations.[10] This overshoot and saturation process can be observed directly in high voltage electron irradiations. A typical example of such experiments is that of Fisher and coworkers on pure copper.[11]

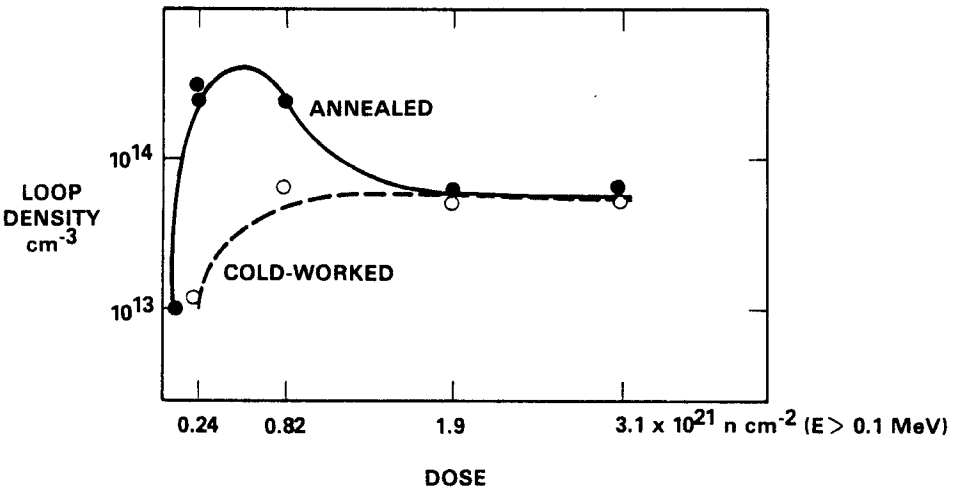

FIGURE 1. Dependence of Dislocation Loop Density on Starting Condition and Fluence in Aluminum Irradiated in the Siloe Reactor at 55°C, as Reported by Risbet and Levy.(10)

The eventual independence of loop number density and mean size on starting cold-work level and fluence have also been demonstrated in AISI 316 by Brager and coworkers [1,5] and is shown in Figures 2 and 3. The strong temperature dependence of the loop density is primarily responsible for the strong temperature dependence of total dislocation density shown in Figure 4.

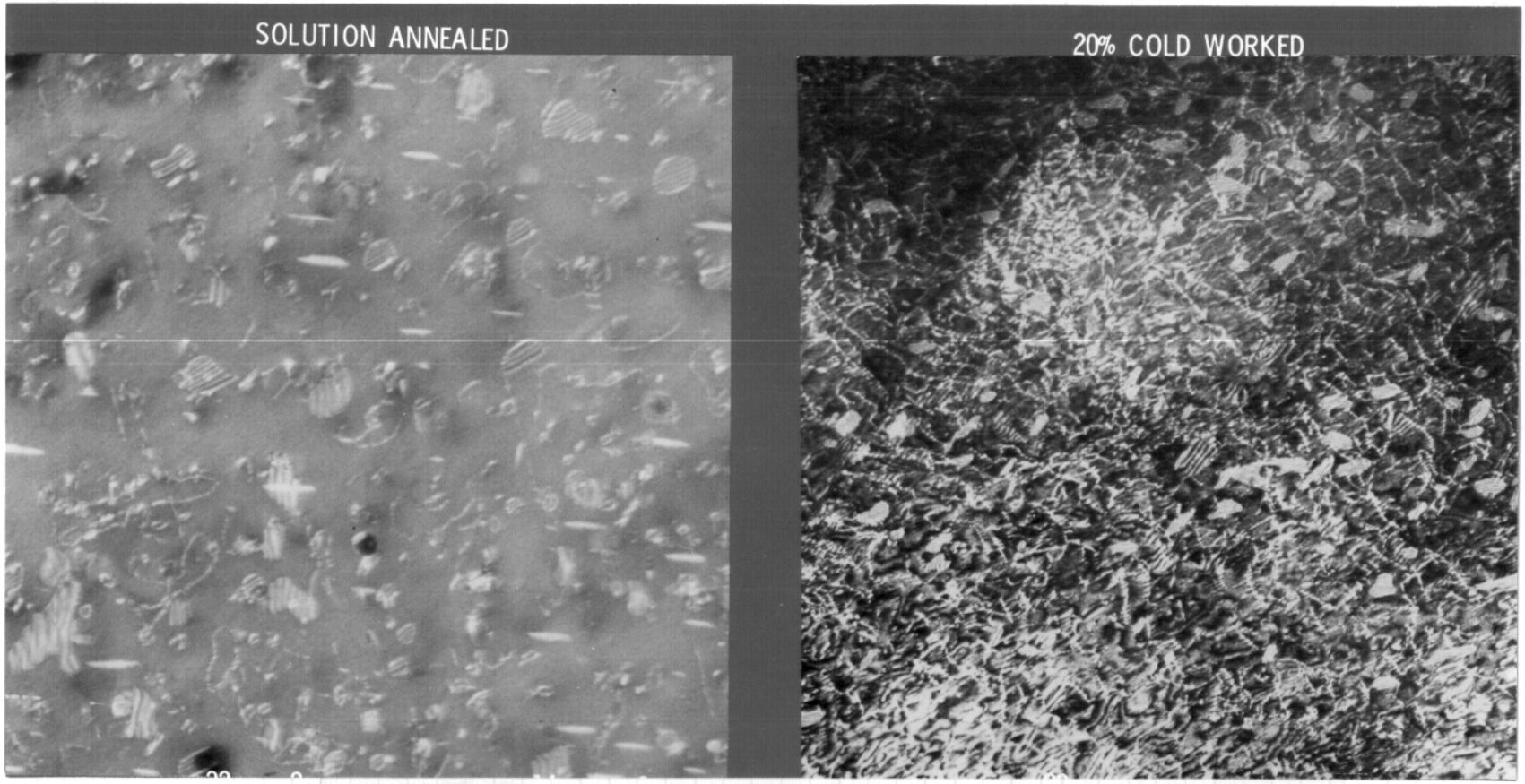

FIGURE 2. Micrographs Showing Dislocation and Loop Microstructures Induced in AISI 316.[5] The annealed specimen contains many Frank loops at 2.0 x 10^{22} n/cm^2 (E >0.1 MeV), with mean size of 372 Å and density 10.2 x 10^{14} cm^3. The 20% cold-worked specimen at 3.0 x 10^{22} n/cm^2 contains a similar density of loops, 11.4 x 10^{14} cm^{-3} with mean size of 424 Å.

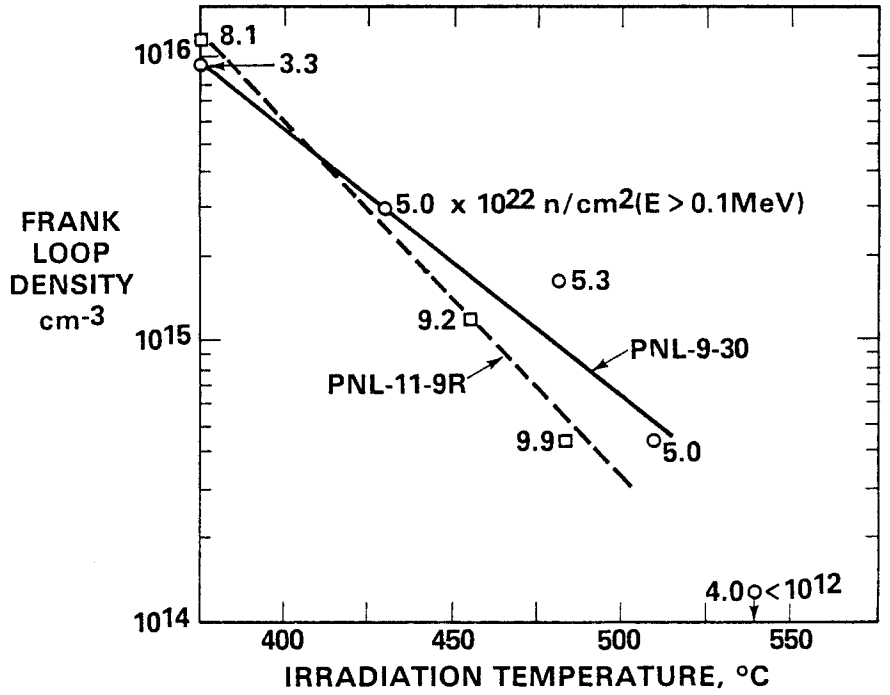

FIGURE 3. Frank Loop Densities Observed in 20% Cold-Worked AISI 316 Fuel Pin Cladding Irradiated in EBR-II. (5) Note that the loop density does not change appreciably with increasing fluence.

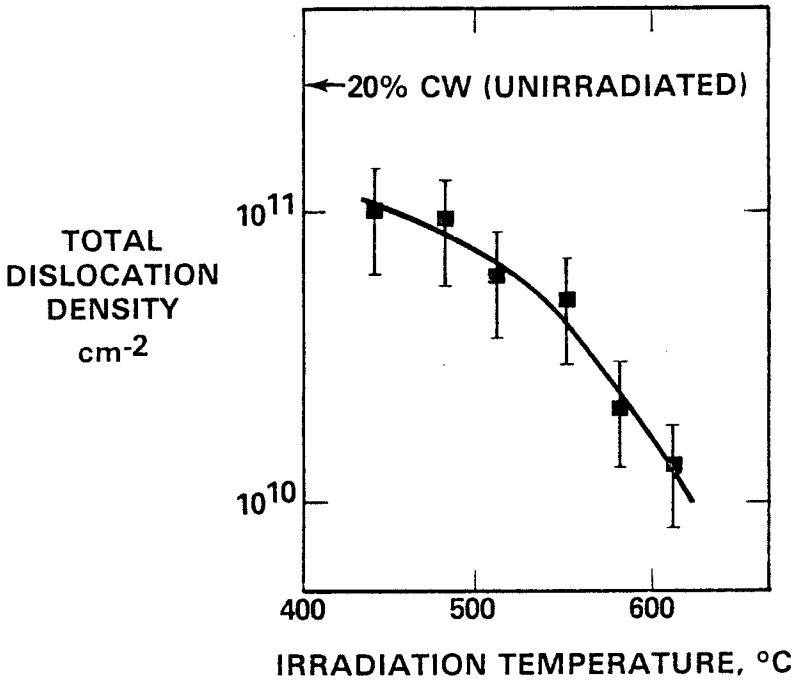

FIGURE 4. Total Dislocation Density Observed in 20% CW M316 Fuel Pin Cladding Designated V1294, as Reported by Bramman and Coworkers. (28) The preirradiation density is also shown.

In effect, the existence of a saturation density of network dislocations leads to a constant intersection probability of Frank loops and a constant rate of production of new line length. Before proceeding then it is necessary to convince ourselves that the network saturation density is indeed relatively insensitive to the pertinent variables in both bulk and surface-affected volumes.

3 Influence of Surface Proximity

It is important to recognize that the saturation dislocation density that evolves will be the result of competing processes of production and loss of line length. In bulk material this process will be unaffected by the loss to specimen surfaces that is characteristic of charged particle irradiations, particularly in relatively soft materials and for ions of shallow penetration. Igata and coworkers [12] have provided a simple depth-independent expression which describes the contribution of surface losses to reduction of the saturation density. They state that the change of dislocation density, ρ, as a function of irradiation time, t, can be expressed as

$$\frac{d\rho}{dt} = S_o - \alpha\rho - \beta\rho^2 \qquad (1)$$

where

ρ = dislocation density,

S_o = dislocation production rate due to radiation,

α = coefficient for rate of dislocation density change due to slip to surface or cross slip due to local internal stress, and

β = coefficient for rate of decrease of dislocation density due to mutual interaction, arising mainly from cross slip or climb motion under irradiation.

At the steady state, the saturation dislocation density ρ_s can be expressed as

$$\rho_s = \frac{-\alpha + \sqrt{\alpha^2 + 4\beta S_o}}{2\beta} \qquad (2)$$

This expression shows that surface losses will reduce ρ_s whenever $\beta S_o > 0$. These losses will be slightly dependent on temperature since the friction stresses experienced by network dislocations are temperature-dependent, thereby increasing the influence of surface image forces. The Frank loops also increase in size with temperature, increasing their probability of intersecting the surface. The proximity of the surface will also tend to reduce S_o in a strongly temperature-dependent manner as point defects are lost to the surface. These three factors will tend to cause the saturation density at high temperatures to fall below the level generated in bulk material.

Despite these losses the dislocation density that evolves in structural metals during ion or electron irradiation experiments is frequently in the same limited range of densities observed in neutron irradiation (10^{10} - 10^{11} cm^3).

4 Review of Network Dislocation Density Data

Figure 5 shows that the dislocation density of both 20% cold-worked and solution annealed AISI 316 converged at a density of 6 ±3 x 10^{10} cm^{-2} at 500°C when irradiated in EBR-II in the absence of stress.[1,5] Figure 6 shows that stressed fuel pin cladding saturated in this density range for temperatures between 375 and 555°C.[1] A similar insensitivity of network dislocation density to starting condition, stress and temperature has been observed in United Kingdom irradiations [13] of M316 (Figure 7) and AISI 316L in the French reactor program [14] (Figure 8).

Hudson has shown (Figure 9) that during irradiation at high displacement rates and far from specimen surfaces the dislocation density saturated at a level just below 10^{11} cm^2 which was relatively insensitive to irradiation temperature and ion identity.[15] Azam and coworkers (Figure 10) demonstrated that even in low energy ion experiments conducted very near foil surfaces that the saturation dislocation density in AISI 316L was approximately 3 x 10^{10} cm^{-2} at 600°C, independent of starting condition and helium content.[14] Similar results have been obtained in low energy ion irradiation of titanium-modified 316 SS.[16]

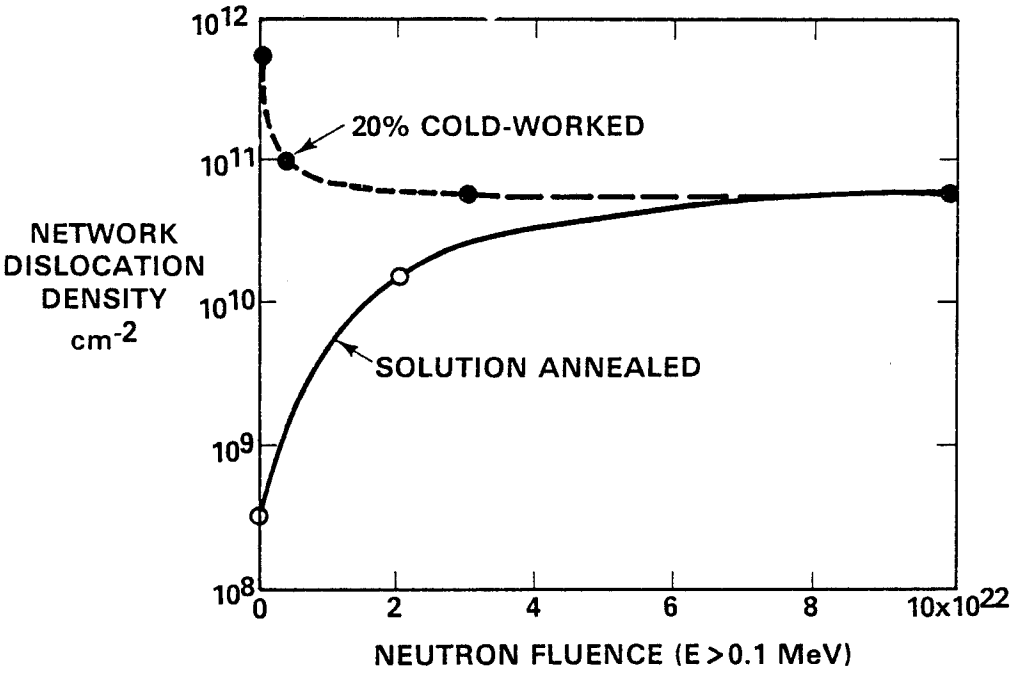

FIGURE 5. Saturation of Network Dislocation Density in Both 20% CW and Annealed AISI 316 After Irradiation in EBR-II. (1)

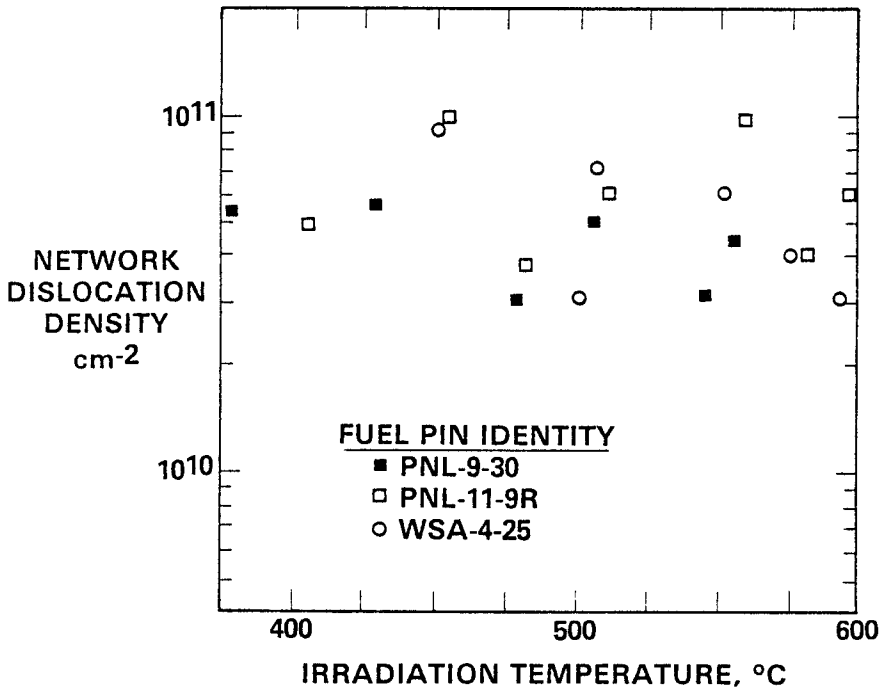

FIGURE 6. Network Dislocation Density Measured in Three 20% CW AISI 316 Fuel Pin Cladding at Doses Ranging from 20 to 50 dpa in EBR-II. (1)

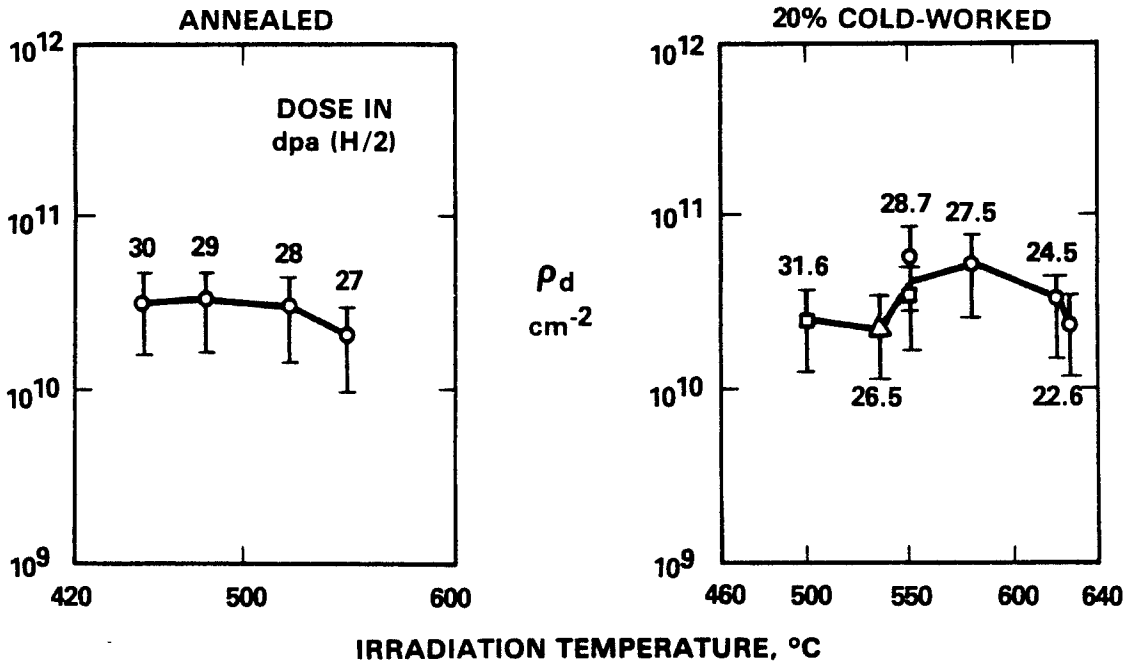

FIGURE 7. Independence of Dislocation Density on Temperature and Starting Condition in M316 Fuel Pin Cladding Irradiated in the Dounreay Fast Reactor as Reported by Brown and Linekar.(13) The numbers beside each data point are the exposure levels in Half-Nelson dpa.

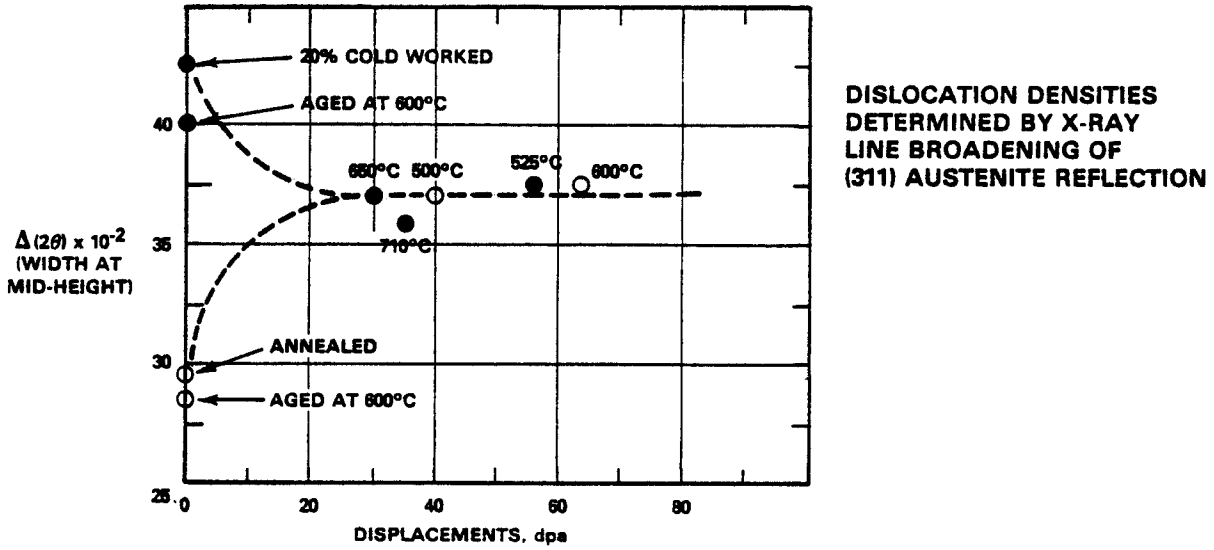

FIGURE 8. Independence of Dislocation Density in AISI 316 on Starting Condition, Temperature and Displacement Level After Irradiation in the Rapsodie Fast Reactor as Reported by Azam, Delaplace and Le Naour.(14) The $\Delta(2\Theta)$ measurement arises from X-ray line broadening measurments on bulk material.

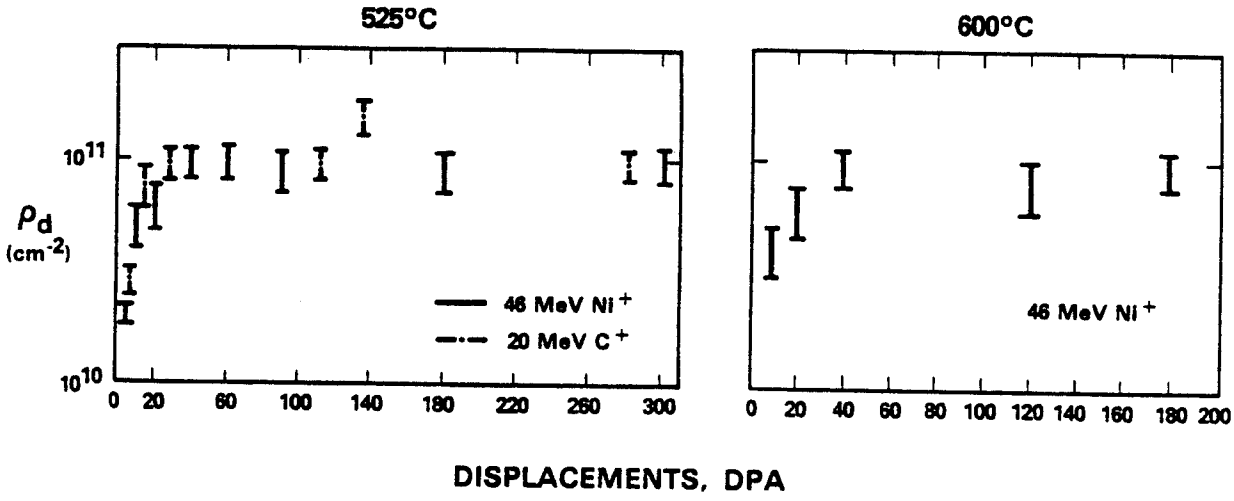

FIGURE 9. Saturation of Dislocation Density at High Displacement Rates in Annealed AISI 316 at 525°C and Annealed 321 at 600°C for Two Deeply Penetrating Ions as Reported by Hudson.(15)

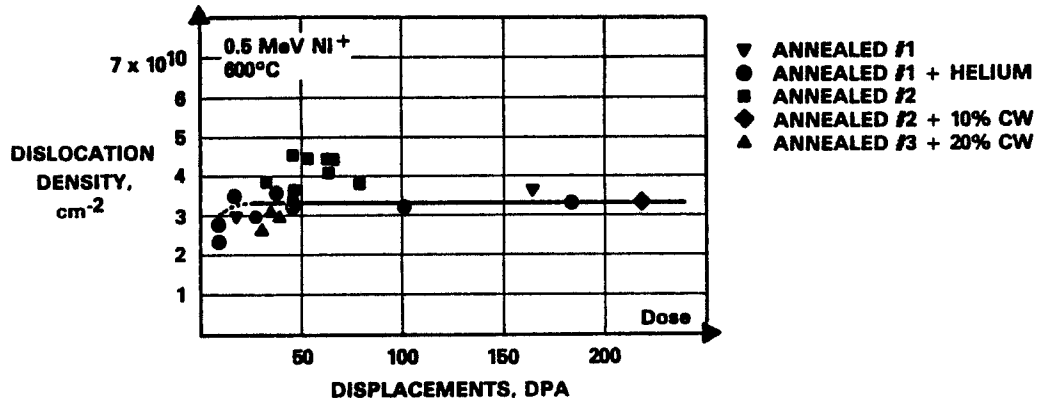

FIGURE 10. Saturation of Dislocation Density at 600°C in Shallow Penetration Ion Bombardment Experiments, Showing Independence of Starting Condition, Heat Identity and Helium Content. Reproduced from Azam, La Naour and Delaplace.(14)

Azam and coworkers also showed that the saturation dislocation density in their surface-affected experiments increased weakly with increasing displacement rate at 600°C. This represents a reduction in the surface influence as S_o in Equation 1 increases and the size of Frank loops decreases. They also demonstrated a weak dependence of saturation density on irradiation temperature in these shallow penetration experiments, reflecting the temperature sensitivity of the coefficient α in Equation 1. The sensitivity of the saturation level to both temperature and displacement rate is shown in Figure 11.

Several groups of researchers have also shown that during dual ion irradiation various alloys develop saturation densities which are relatively insensitive to the helium/dpa ratio and to the mode and schedule of helium injection.[17-20] An example of this behavior for a soft alloy without solute is shown in Figure 12. The low saturation level of $\sim 2 \times 10^{10}$ cm^{-2} reflects the soft nature of the alloy and the proximity of the surface.

5 A Model for the Evolution of Network Dislocation Density in Irradiated Metals

It has been shown that the saturation network dislocation density that evolves at high fluence in irradiated bulk metals is remarkably insensitive to temperature, displacement rate, stress, helium content or starting microstructure. The major features of this evolution are shown in Figure 13 and can be described as being the result of the competitive action of two primary mechanisms in a material where there are no additional losses of dislocation line length to surfaces or substantial losses to grain boundaries. These two primary mechanisms are (a) generation of line length by loop growth and interaction with other components of the network and (b) recovery processes involving annihilation of line length.

6 Description of Recovery Processes

Both thermally activated and radiation-induced climb of edge dislocation lead to encounters of dislocations, some of which result in annihilation of line

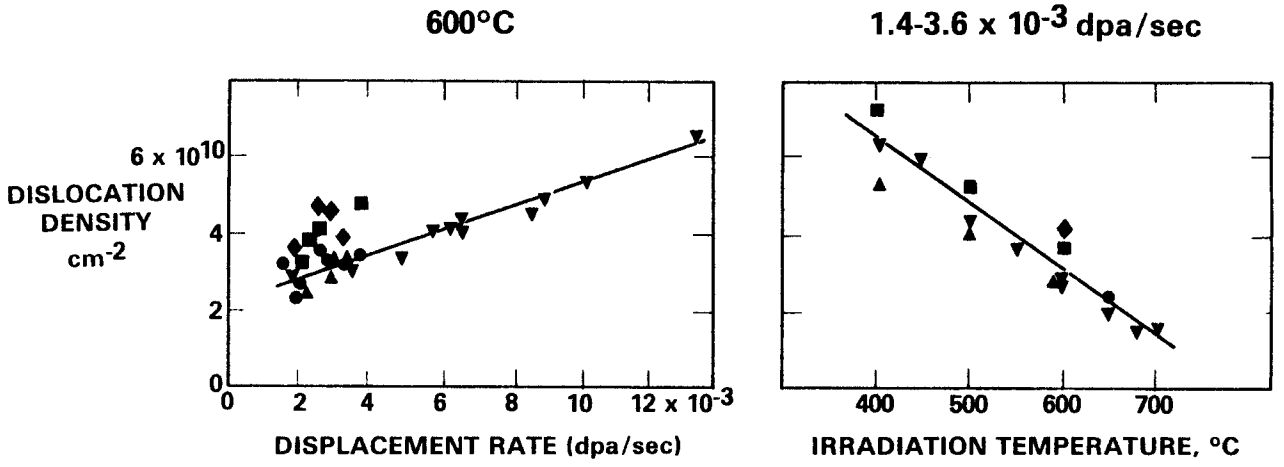

FIGURE 11. Dependence of Saturation Dislocation Density on Surface Influence, as Demonstrated by Dependence of Dislocation Density on Temperature and Displacement Rate.(14) All symbols are defined in Figure 10.

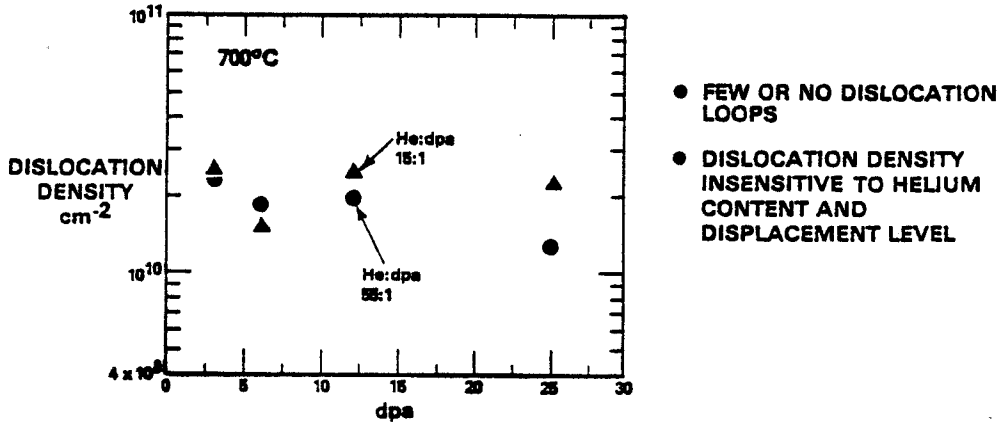

FIGURE 12. Dislocation Saturation Level is Independent of Helium Content in Dual Ion Irradiations of Fe-20Ni-15Cr at 700°C as Reported by Agarwal and Coworkers.(19) According to Agarwal, preinjected specimens (15 appm, not shown) attained the same dislocation density.

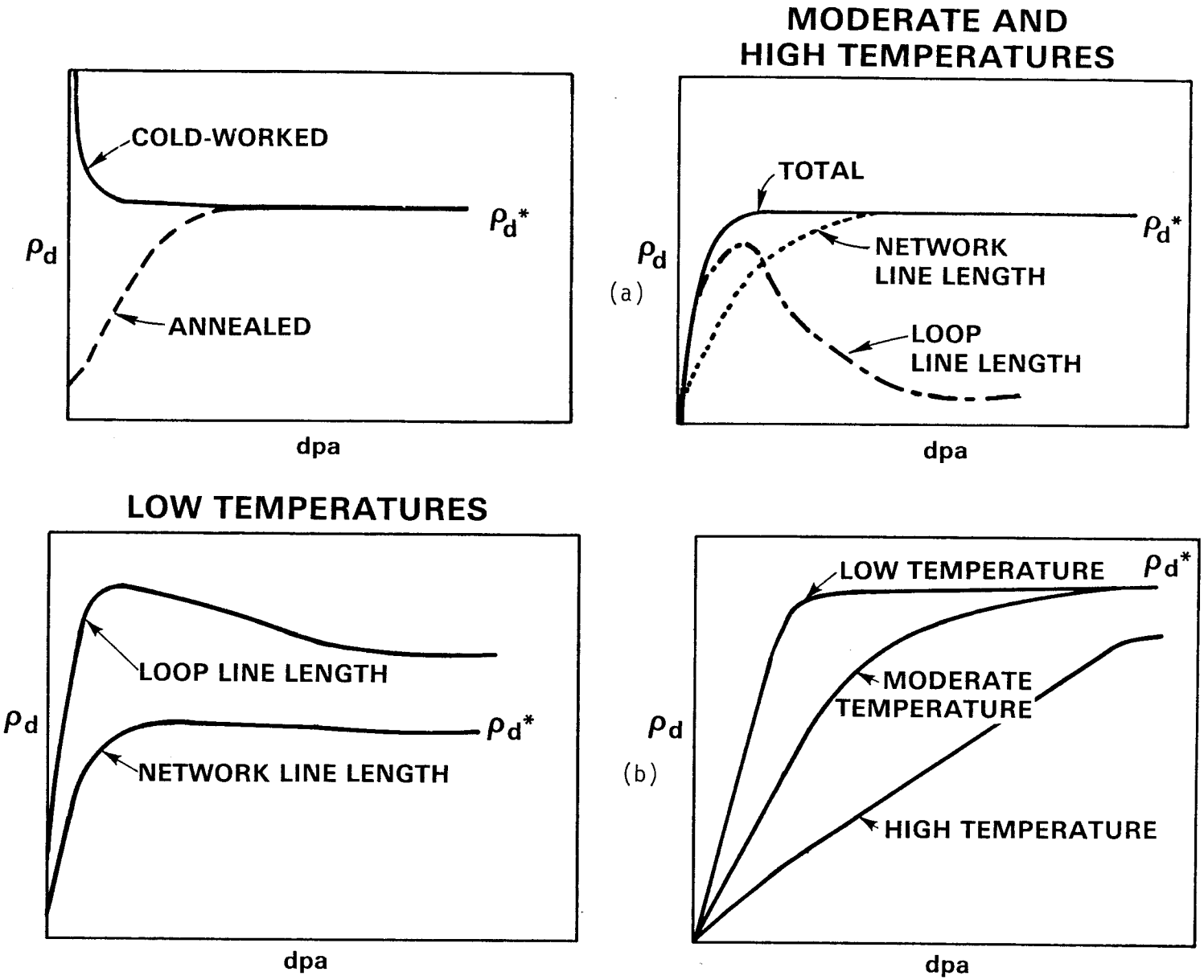

FIGURE 13. Schematic Representation of Dislocation Network Evolution in Metals Without Surface Influence.

length and recovery. The rate of annihilation of the network dislocation density ρ is commonly assumed to be proportional to ρ^2 in recovery models for thermal creep. The same assumption is expressed in Equation 1. The ρ^2 dependence is based on the simple argument that the chance encounter of two edge dislocations with opposite Burgers vectors on the same glide plane is proportional to ρ^2. This assumption is only appropriate when the motion of edge dislocations by climb and glide is completely random.

On the other hand, in the absence of large creep deformations, the motions of adjacent edge dislocations are actually correlated during radiation-induced recovery. Consider, for example, the simple model of an edge dislocation structure shown in Figure 14a. Numerous edge dislocations can be paired up into dislocation dipoles, i.e., closest pairs of parallel edge dislocations with opposite Burgers vectors on parallel glide planes. As a result of radiation-induced climb, a pair may either increase or decrease the distance h(t) between the parallel glide planes. When h(t) increases, the members of the pair become partners in other dipole configurations until eventually they pair up in such a way that the corresponding values of the glide plane separation h(t) decrease with time. As a result, the members of approaching pairs eventually interact primarily with each other, and the orientation of the dipole tends to remain at an angle of 45° (the minimum energy configuration) to the glide plane as h(t) decreases further. Subsequent motion by climb and glide is then completely correlated.

This argument can be made more general by stating that the configuration of continuously climbing dislocations is determined by their mutual interaction, and that the network will always adjust by glide to minimize the total elastic interaction energy of the network. Again, glide and climb motions are correlated.

In order to arrive at the rate of annihilation of network dislocations consider the dislocation array shown in Figure 14a. The number of adjacent dislocations able to form dipoles is obviously $\rho/2$. On the average the time required for the two dislocations to climb to a common glide plane is equal to $\tau = h_o/2V$,

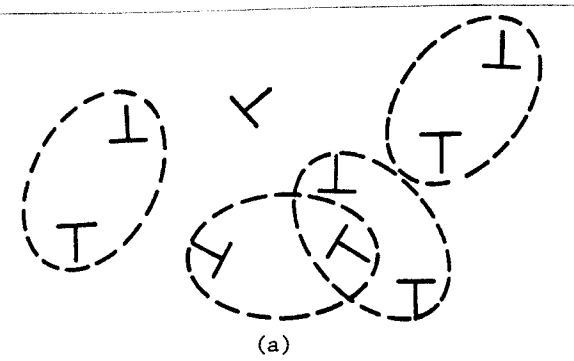

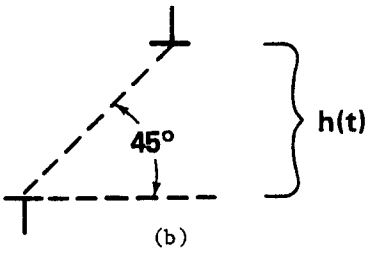

FIGURE 14. Schematic Representation of Correlated Movement of Dislocation Pairs (dipoles).

where h_o is the initial dipole separation distance and V the dislocation climb velocity. Consequently, the rate of annihilation is $(\rho/2)/\tau$ or $\rho V/h_o$. On the average, we may assume that $\pi h_o^2 = 1/\rho$, so that the annihilation rate is equal to $\sqrt{\pi}\, V\, \rho^{3/2}$.

7 Description of Generation Processes

The generation of network dislocations by the formation, growth, coalescence and unfaulting of Frank loops is a complicated process. However, several facts can be utilized to simplify matters for this derivation.

First, detailed computer solutions by many authors [21-25] have shown that formation of an interstitial loop occurs very quickly, requiring only a few seconds of irradiation. Furthermore, both coalescence and unfaulting of loops are relatively fast processes in comparison to that of loop growth. As a result, the generation of network dislocations occurs at a rate dictated by the lifetime τ_ℓ of an interstitial loop, defined as the period from its formation to its coalescence with other components of the network. If R(t) is the radius of a loop, its growth rate can be calculated by differentiating the expression describing the growth rate of loop area and is given by

$$dR/dt = b^2[Z_i^\ell D_i C_i - Z_v^\ell D_v C_v + Z_v^\ell D_v C_{vo}^\ell] , \quad (3)$$

where b is the Burgers vector, Z_i^ℓ and Z_v^ℓ the loop bias factors, D_i and D_v the diffusion coefficients, and C_i and C_v the concentrations for interstitials and vacancies, respectively. C_{vo}^ℓ is the vacancy concentration in thermodynamic equilibrium with the loop.

If Equation 3 is written in the abbreviated fashion

$$\frac{dR}{dt} = b^2 \Phi , \quad (4)$$

then Φ is a function which depends on displacement rate, stress, temperature and the total sink density according to conventional rate theory. After the first generation of loops has been formed, it is no longer dependent on the individual loop radii. Hence Equation 4 can be integrated to obtain the loop lifetime as

$$\tau_\ell = \overline{R_{max}}/b^2 \Phi , \quad (5)$$

where $\overline{R_{max}}$ is the average maximum loop radius in a quasi-stationary population.

Brager, Garner and Guthrie [5] have shown that $\overline{R_{max}}$ is proportional to $\rho^{-\frac{1}{2}}$ in well-developed microstructures at high fluence. Therefore, the generation rate of dislocations is proportional to $1/\tau_\ell$ or $b^2\Phi\rho^{\frac{1}{2}}$.

8 The Evolution of Network Dislocation Density

Assuming no other losses the rate of change of dislocation density is

$$\frac{d\rho}{dt} = B\rho^{\frac{1}{2}} - A\,\rho^{3/2} , \qquad (6)$$

where

$$B \sim b^2\Phi$$

and

$$A \sim V = b^2[Z_i^d D_i C_i - Z_v^d D_v C_v + Z_c^d D_v C_{vo}^d] + V_{th} . \qquad (7)$$

Apart from the different bias factors for edge dislocations, Z_i^d and Z_v^d, and the different thermal vacancy concentration C_{vo}^d in equilibrium with the edge dislocation, the radiation-induced contribution to the climb velocity V is very similar to the average loop growth rate $b^2\Phi$.

In fact, the loop bias factors as well as C_v^ℓ differ from the corresponding values for edge dislocations only for small loop radii (less than 50 Å).[7] Therefore, B is essentially proportional to the loop growth rate in Equation 4. Note that in a saturation network the size distribution of loops is invariant,[7-8] and thus the ratios Z_i^ℓ/Z_i^d and Z_v^ℓ/Z_v^d are also invariant.

The second term in this equation, V_{th}, represents the thermally induced climb rate which determines the rate of recovery in the absence of radiation. Since thermal recovery is significant only at temperatures above 650°C for typical fast reactor irradiation, it can be neglected at lower irradiation temperatures.

At higher displacement rates the temperature at which V_{th} becomes important tends to increase as the microstructural densities undergo an upward shift in temperature.

Therefore, there is some relatively high temperature (dependent on displacement rate) below which the ratio B/A becomes a constant independent of the various sink densities. The strong temperature dependence of both A and B cancels, yielding a temperature-independent value of B/A. The saturation dislocation density, defined by $d\rho/dt = 0$ is

$$\rho_S = B/A \ . \tag{8}$$

This means that below the temperature where V_{th} is important the saturation density is not only independent of temperature and the details of the temperature-dependent microstructure but also independent of the starting microstructure. Since stress also makes no substantial changes in terms of Equations 3 and 7 at temperatures where V_{th} is unimportant, this means that the saturation density should also be essentially independent of stress. This independence also explains why ion bombardment experiments reach the same saturation range as do unstressed neutron irradiation experiments. The differential swelling inherent in ion irradiations leads to large levels of stress in the irradiated region of the foil.[26-27] It has been shown, however, that the application of stress to irradiated metals speeds up the early evolution toward the saturation state.[1,5,7]

The solution to Equation 6 is given by

$$\rho(t)/\rho_s = \frac{1 - e^{-x} + \sqrt{\rho_o/\rho_s}\,(1 + e^{-x})}{1 + e^{-x} + \sqrt{\rho_o/\rho_s}\,(1 - e^{-x})} \ , \tag{9}$$

where ρ_o is the initial dislocation density and

$$x = A\sqrt{\rho_s}\ t$$

$$= \sqrt{\Pi\rho_s}\ Vt \tag{10}$$

Since A and V are dependent on temperature, the approach to the saturation level ρ_s is also dependent on temperature.

Using a saturation dislocation density of 6×10^{10} cm^{-2},[1] an initial dislocation density of 4×10^{8} cm^{-2} for annealed 316 and 7×10^{11} cm^{-2} for 20% CW 316, the fluence-dependent dislocation densities according to Equation 9 are shown in Figure 15. The relationship between fluence and the variable x was chosen such that the dislocation density for annealed 316 reaches the value of 2×10^{10} cm^{-2} at 2×10^{22} n/cm^2, as reported for AISI 316 irradiated in EBR-II at 500°C.[7] This fluence value corresponds to x = 1.2, so that

$$x = \frac{0.6\ \phi t}{10^{22}} \tag{11}$$

where the fluence is given in units of n/cm^2 (E >0.1 MeV).

The dislocation climb velocity V was also computed according to rate theory for a displacement rate of 1.0×10^{-6} dpa/s. The results are shown in Figure 16. At low temperature, recombination of point defects results in a reduced climb velocity. Since the dislocation bias decreases slightly with temperature, the climb velocity also decreases at high temperatures.

It is seen from Figure 16 that the climb velocity is proportional to the bias difference between dislocations in different configurations. Dislocation climb occurs even in the absence of voids as a result of these bias differences. Assuming that 1% difference in bias is a typical value, it is possible to compute independently according to Equation 10 the relationship betweel the fluence and the variable x. At 500°C, the climb velocity is computed to be V = 1.0 Å/dpa, or for a displacement rate of 1.0×10^{-6} dpa/s, V = 10^{-12} cm/s. Hence

$$x = \sqrt{\pi\rho_s}\ Vt = \sqrt{\pi\rho_s}\ \frac{V}{\phi}\ \phi t$$

$$= 1.74 \times 10^{-22}\ \phi t \tag{12}$$

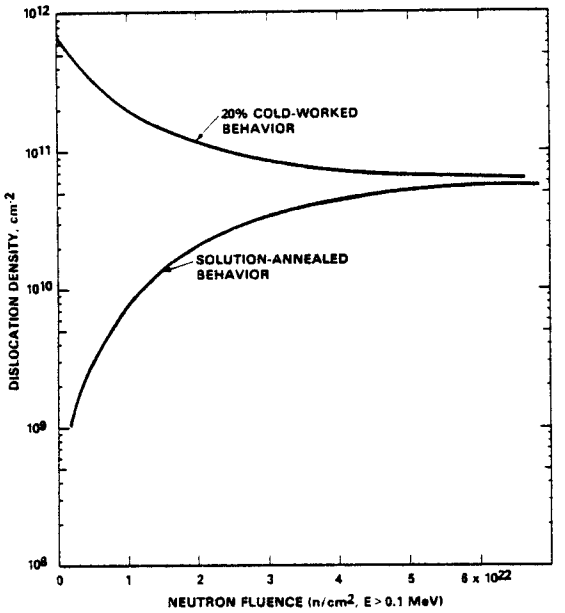

FIGURE 15. Predictions of the Evolution of Dislocation Density in AISI 316 at 500°C for Starting Densities of 7×10^{11} cm/cm^3 and 4×10^8 cm/cm^3, Chosen to Represent Cold-Worked and Annealed Conditions.

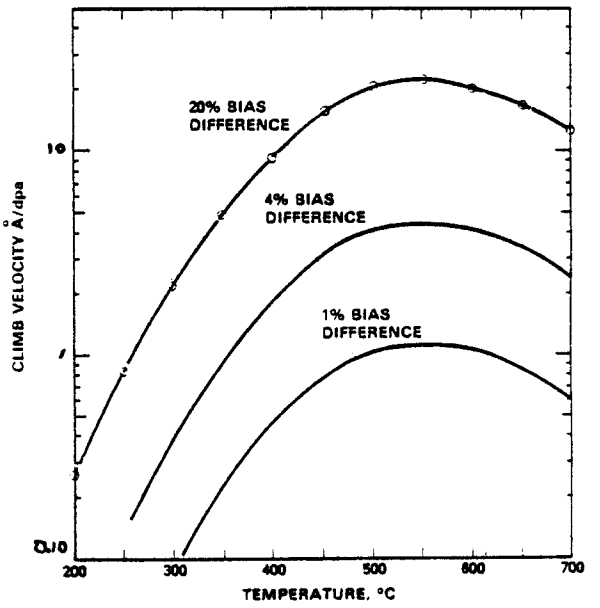

FIGURE 16. Calculation of Dislocation Climb Velocity V for Several Values of Bias Difference Between Dislocations in Different Configurations. The displacement rate was assumed to be 10^{-6} dpa/sec.

assuming a neutron flux of 2.5×10^{15} n/cm^{2}s. The numerical factors in Equations 11 and 12 are equal within 10%.

9 Conclusions

It appears that it is possible to explain how the rate of approach to the saturation density of network dislocations is dependent on temperature but the eventual saturation level is not. The model developed to explain this apparent contradiction also predicts an independence of saturation level on starting microstructure, stress and displacement rate below temperatures where thermal emission of vacancies from dislocations becomes an important factor in their climb rate.

References

1. H. R. Brager, F. A. Garner, E. R. Gilbert, J. E. Flinn and W. G. Wolfer, "Stress Affected Microstructural Development and the Creep-Swelling Relationship," in Radiation Effects in Breeder Reactor Structural Materials, M. L. Bleiberg and J. W. Bennett, Eds., The Metallurgical Society of AIME, 1977, p. 727.

2. G. D. Johnson, F. A. Garner, H. R. Brager and R. L. Fish, "A Microstructural Interpretation of the Fluence and Temperature Dependence of the Mechanical Properties of Irradiated AISI 316," Effects of Irradiation on Materials: Tenth Conference, ASTM STP 725, D. Kramer, H. R. Brager and J. S. Perrin, Eds., 1981, pp. 393-412.

3. F. A. Garner, M. L. Hamilton, N. F. Panayotou and G. D. Johnson, J. Nucl. Mater., 103 and 104 (1981) 803-808.

4. P. R. Okamoto and S. D. Harkness, J. Nucl. Mater., 48 (1973) 49.

5. H. R. Brager, F. A. Garner and G. L. Guthrie, J. Nucl. Mater., 66 (1977) 301.

6. F. A. Garner and W. G. Wolfer, Trans. Am. Nucl. Soc., (1978) 144.

7. F. A. Garner, W. G. Wolfer and H. R. Brager, "A Reassessment of the Role of Stress in Development of Radiation Induced Microstructure," in Effects of Radiation on Structural Materials, ASTM STP 683, J. A. Sprague and D. Kramer, Eds., ASTM, 1979, pp. 160-183.

8. D. S. Gelles, F. A. Garner and H. R. Brager, "Frank Loop Formation in Irradiated Metals in Response to Applied and Internal Stresses," Effects of Radiation on Materials: Tenth Conference, ASTM STP 725, K. Kramer, H. R. Brager and J. S. Perrin, Eds., ASTM, 1981, pp. 735-753.

9. A. Si-Ahmed and W. G. Wolfer, "On the Simultaneous Formation of Interstitial and Vacancy Loops During Irradiation," in Dislocation Modeling of Physical Systems, M. F. Ashby, R. Bullough, C. S. Hartley and J. P. Hirth, Eds., Pergamon Press, 1980, p. 142.

10. A. Risbet and V. Levy, J. Nucl. Mater., 46 (1973) 341.

11. S. B. Fisher, R. J. White and K. M. Miller, Phil. Mag. A, 40 (1979) No. 2, p. 239.

12. N. Igata, A. Kohyama and S. Nomura, "Void Swelling in Molybdenum Alloys In-Situ Observed by a High Voltage Electron Microscope," in Ref. 2, p. 627.

13. C. Brown and G. Linekar, "Dislocation Densities in ST and 20% Cold-Worked Type 316 Pin Cladding Irradiated to 30 dpa in PFR," UKAEA TRG-Memo-6571, June 1974.

14. N. Azam, L. Le Naour and J. Delaplace, J. Nucl. Mater., 49 (1973/74) 197.

15. J. A. Hudson, J. Nucl. Mater., 60 (1976) 89.

16. H. Kawanishi, M. Yamada, K. Fukuya and S. Ishino, J. Nucl. Mater., 103 and 104 (1981) 1097.

17. N. H. Packan and K. Farrell, J. Nucl. Mater., 85 and 86 (1979) 677.

18. K. Farrell and N. H. Packan, ibid, p. 683.

19. S. C. Agarwal, G. Ayrault, D. I. Potter, A. Taylor and F. V. Nolfi, Jr., ibid, p. 653.

20. J. A. Spitznagel and A. P. L Turner, Proceedings of Damage Analysis and Fundamental Studies Information Meeting, October 2-3, 1981, p. 298.

21. M. R. Hayns, J. Nucl. Mater., 56 (1975) 267.

22. R. A. Johnson, J. Nucl. Mater., 75 (1978) 77.

23. N. M. Ghoniem and D. D. Cho, Phys. Stat. Sol. (A), 54 (1979) 171.

24. B. O. Hall, J. Nucl. Mater., 91 (1980) 63.

25. N. M. Ghoniem and S. Sharafat, J. Nucl. Mater., 92 (1980) 121.

26. F. A. Garner, G. L. Wire and E. R. Gilbert, in Proceedings of International Conference on Radiation Effects and Tritium Technology for Fusion Reactors, Gatlinburg, TN, 1975, CONF-750989, p. 474.

27. W. G. Wolfer and F. A. Garner, J. Nucl. Mater., 85 and 86 (1979) 583.

28. J. I. Bramman, C. Brown, J. S. Watkin, C. Cawthorne, E. J. Fulton, P. J. Barton and E. A. Little, "Void Swelling and Microstructural Changes in Fuel Pin Cladding and Unstressed Specimens Irradiated in DFR," in Ref. 1, pp. 479-507.

Acknowledgment

Support for this work has been provided by the U.S. Department of Energy under contracts DE-AC14-76FF02170 with the Hanford Engineering Development Laboratory and under contract DE-AC02-82ER52082 with the University of Wisconsin.